NUMERICAL SIMULATION OF NEGATIVE STREAMERS IN STRONG NON-UNIFORM ELECTRIC FIELDS IN NITROGEN. EFFECT OF NEEDLE RADIUS AND APPLIED VOLTAGE ON STREAMER VELOCITY

O.V. Manuilenko, V.I. Golota
National Science Center "Kharkov Institute of Physics and Technology", Kharkov, Ukraine
E-mail: ovm@kipt.kharkov.ua

The results of numerical simulations of the propagation of a negative streamer in nitrogen in the uniform and strongly non-uniform electric fields are presented. It is shown that the propagation velocity of the streamer in a non-uniform electric field is always higher than its velocity in an uniform field at given voltages on electrodes. It is shown that as the needle radius decreases, the velocity of the streamer increases. The growth of streamer velocity, with decrease of the needle radius, is stopped when the needle curvature radius reaches a certain critical size. It is shown that in the region of the strong nonlinearity, when the streamer dynamics is determined by the charge of the streamer head, its velocity as a function of the longitudinal coordinate is independent of the needle radius. It is shown that the velocity of the streamer increases with growth of the applied voltage.

PACS: 52.80.Mg, 52.80.Tn

INTRODUCTION

Papers [1 - 5] are devoted to the numerical modeling of the negative streamer in nitrogen within the drift - diffusion approximation. In these works, with the exception of [5], the regular nonadaptive meshes to solve the continuity and Poisson equations are used. Streamer is a nonlinear structure with a sharp edge. Therefore, for its correct resolution in numerical simulations the exponential representation for the current density in the drift-diffusion approximation - the Scharfetter-Gummel algorithm [6], or numerical schemes with adaptation of a regular grid [5] were used. Regular meshes, as opposed to irregular grids, which are used in the finite element method, can not accurately describe the arbitrary boundaries of complex shape, such as the needle - to - plane. Therefore, the finite element method was used in our simulations.

The computer simulations of the negative (anode - directed) streamers in nitrogen in the uniform (plane - to - plane geometry) and non-uniform (needle - to - plane geometry) fields are presented in [7, 8]. The effect of the needle radius on the negative streamer speed has been studied just for one electrode potential. It has been shown that the velocity of the negative streamer in a nonuniform electric field is higher than its velocity in a uniform field. It has been shown that as the radius of the needle decreases, the streamer velocity increases.

The results of numerical simulations of negative streamer dynamics in nitrogen, using the finite element method (SUPG, CWDPG), are presented below. The computer simulations were performed for uniform and non-uniform electric fields. The effect of applied voltages at different radii of the needle on the streamer speed is investigated.

1. MODEL

The set of equations describing the propagation of the negative (anode - directed) streamer in nitrogen is:

$$\frac{\partial n_e}{\partial t}+\nabla\cdot\left(-n_e\mu_e\vec{E}-D_e\nabla n_e\right)=S_{iz}, \qquad (1)$$

$$\frac{\partial n_i}{\partial t}+\nabla\cdot\left(n_i\mu_i\vec{E}-D_i\nabla n_i\right)=S_{iz} \qquad (2)$$

$$\nabla^2 V=\frac{e}{\varepsilon_o}\left(n_e-n_i\right), \qquad \vec{E}=-\nabla V, \qquad (3)$$

where n_e n_i are the number densities for electrons and positive ions, μ_e, μ_i are the electron and ion mobilities, D_e, D_i are the diffusion coefficients for electrons and ions. V is the potential of electric field, e is the electron charge, ε_o is the permittivity of free space. S_{iz} is the rate of charged particle generation due to collisional ionization:

$$S_{iz}=n_e\mu_e\,|\,\vec{E}\,|\,\alpha_o\exp\left(-E_o/\left|\vec{E}\right|\right), \qquad (4)$$

where α_o is the ionization coefficient, E_o is the threshold field for impact ionization. In the right hand sides of equations (1) and (2) other sources and sinks of charged particles, such as, photoionization and recombination, were not included. These sources and sinks are negligible, compared to the impact ionization, for pure nitrogen on the simulation time (streamer propagation time through the discharge gap).

Expression (4) allows the introduction of a set of natural scales: spatial scale $l_o=1/\alpha_o$, electric field scale E_o, velocity scale $v_o=\mu_e E_o$, time scale $t_o=l_o/v_o$, diffusion scale $D_o=l_o^2/t_o$, and density scale $n_o=\varepsilon_o\cdot E_o/\left(e\cdot l_o\right)$. For nitrogen, under normal conditions, E_o = 197600 V/cm, α_o=4332 cm^{-1}, μ_e=460 cm^{2}V^{-1}s^{-1}. Passing in (1) - (3) to dimensionless variables $\vec{r}=\vec{r}/l_o$, $t=t/t_o$, $n_e=n_e/n_o$, $n_i=n_i/n_o$, the following equations can be obtained:

$$\frac{\partial n_e}{\partial t}+\nabla\cdot\left(-n_e\vec{\varepsilon}-D\nabla n_e\right)=n_e\,|\,\vec{\varepsilon}\,|\exp\left(-\frac{1}{|\,\vec{\varepsilon}\,|}\right), \qquad (5)$$

$$\frac{\partial n_i}{\partial t}=n_e\,|\,\vec{\varepsilon}\,|\exp\left(-\frac{1}{|\,\vec{\varepsilon}\,|}\right), \qquad (6)$$

$$\nabla^2 V=n_e-n_i\equiv-\rho, \qquad \vec{\varepsilon}=-\nabla V. \qquad (7)$$

Ions in (6) are further considered as immovable, since their mobility is several orders of magnitude smaller than the electron mobility, which allows neglecting their displacement for the simulation time.

Fig. 1 shows the simulation domain, example of mesh for solution of (5) - (7) and the boundary conditions. Initially electrons and ions are located at the cathode with number densities: $n_e = n_i = \delta \cdot \exp\left(-\vec{r}^{\,2}/\sigma\right)$, δ =10^{-4}, σ =100. The potential of the anode changed in simulations: V_0 = {96, 128, 160, 192}, which corresponds for the plane - to - plane geometry approximately to {74.1, 98.8, 123.5, 148.2} kVcm^{-1}. Dimensionless diffusion coefficient is D = 0.1, which corresponds to 1800 cm^{2}s^{-1}. The other parameters are: L_z =256, L_r = 128, H = 40, needle radius is one of R_n ={20, 40, 80, inf}. R_n = inf means uniform electric fields, or plane - to - plane simulation domain. For the plane - to - plane computation domain $R_n + H_{ndl}$ =0.

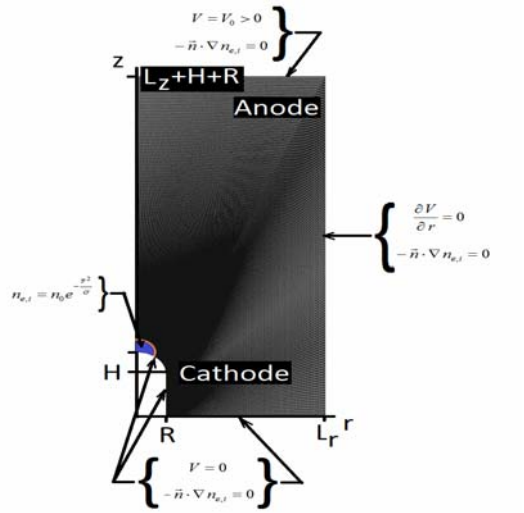

Fig. 1. Simulation domain and boundary conditions

2. SIMULATION RESULTS

Figs. 2, 3 show, for example, the computer simulation results of the avalanche - to - streamer transition, and the propagation of negative streamer through the discharge gap with the uniform (left column) and non - uniform (right column) electric fields. R_n = 20. V_0 = 128. Fig. 2 shows distribution of the space charge density $\rho(r,z;t)$ in $\{r,z\}$ at different times. Fig. 3 presents the distribution of the absolute value of the electric field $\left|\vec{\varepsilon}(r,z;t)\right|$ at the same time points. The time points are chosen so that the streamer in the uniform and non-uniform field advanced the same distance. For the uniform field these time points are t = {115, 175, 200}, and for the non-uniform field these time points are t = {50, 100, 125}.

As can be seen from Figs. 2 and 3, in the inhomogeneous field the streamer has a larger transverse dimension, higher speed and smaller forming time. In both cases, the electric field is enhanced in front of the streamer head, and weakened behind it.

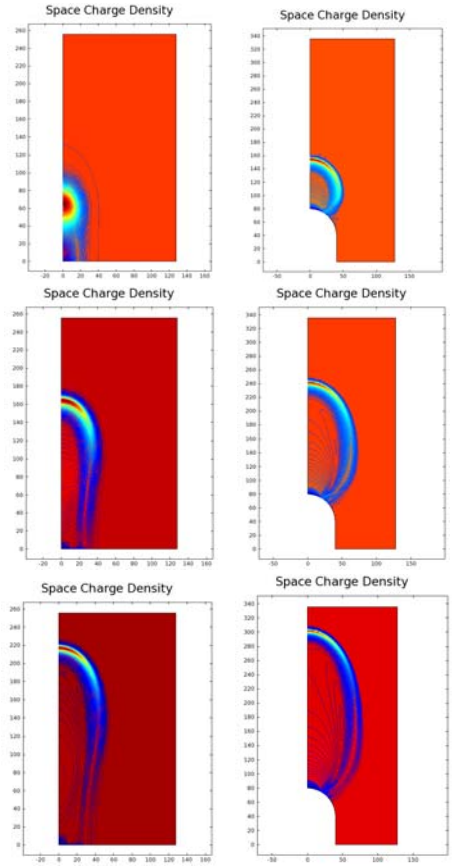

Fig. 2. Space charge density $\rho(r,z;t)$.
Left column - uniform electric field.
Right column - non - uniform electric field

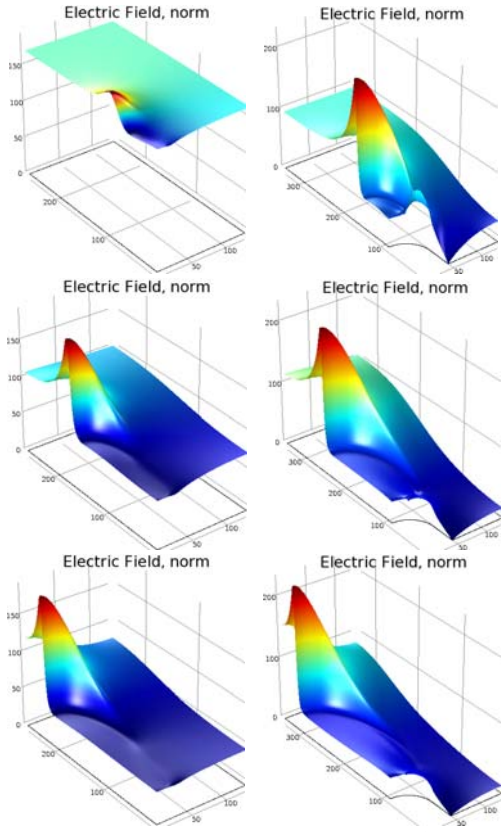

Fig. 3. Absolute value of the electric field $\left|\vec{\varepsilon}(r,z;t)\right|$.
Left column - uniform electric field.
Right column - non - uniform electric field

ISSN 1562-6016. ВАНТ. 2013. №4(86)

Fig. 4 shows the absolute value of the electric field $|\vec{\varepsilon}(r=0,z;t)|$, and the space charge density $\rho(r=0,z;t)$ on the axis depending on the longitudinal coordinate z at different time points $t=[0,130]$ with the step $dt=5$. R_n = 20 and V_0 = 128. As can be seen from Fig. 4, the vacuum (Laplacian) electric field of the needle is quickly screened by the streamer. The electric field $|\vec{\varepsilon}(r=0,z;t)|$, as well as the space charge density $\rho(r=0,z;t)$, changes weakly when the streamer moves through the discharge gap. When the streamer head approaches the anode, this increases the local electric field in front of the streamer head, and leads to the growing collisional ionization rate. This increases the densities of charged particles and the space charge density $\rho(r=0,z;t)$. It can be seen that the head of the negative streamer, as it moves towards the anode, is compressed in the longitudinal direction.

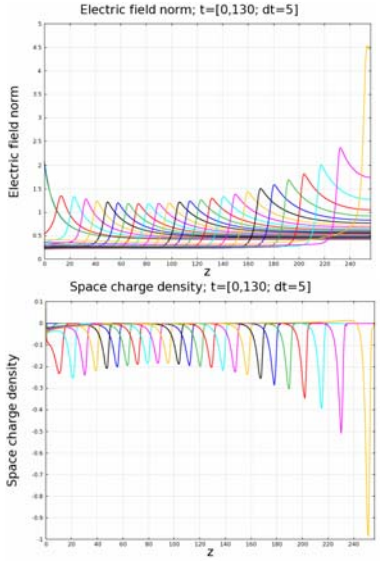

Fig. 4. Electric field $|\vec{\varepsilon}(r=0,z;t)|$ and space charge density $\rho(r=0,z;t)$ on the axis at different times

Fig. 5 (left column) shows the z-coordinates of the maximum of the electric field $|\vec{\varepsilon}(r=0,z;t)|^{\max}$ on the axis as the function of time for different values of the needle radii R_n = {20, 40, 80, inf}, and the anode potentials V_0 = {96, 128, 160, 192}. R_n = inf means uniform electric fields, or plane - to - plane computational domain. Fig. 5 (right column) shows the velocity of $|\vec{\varepsilon}(r=0,z;t)|^{\max}$ versus time, which is the negative streamer propagation velocity through the discharge gap - V_s. As seen from Fig. 5, the streamer velocity increases as the needle radius decreases. This increase in the velocity goes up to a certain radius ($R_n \sim 40$), after which the growth of streamer speed is cut off. As can be seen from Fig. 5, the behavior of streamer velocity V_s as a function of time has four characteristic regions: (1) the sharp drop at the beginning of the movement, (2) the motion with a nearly constant velocity, (3) the region of the first (low) acceleration, and (4) the region of the second (strong) acceleration.

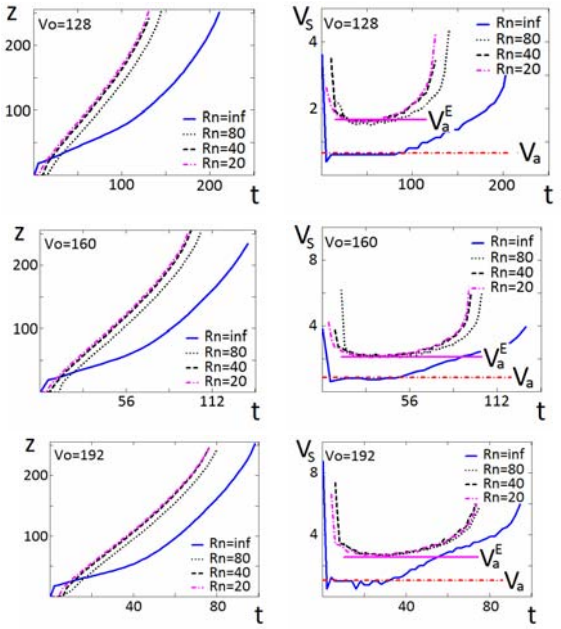

Fig. 5. Negative streamer dynamics for different radii of the needle R_n ={20, 40,80, inf} and different applied voltages V_0 = {96, 128, 160, 192}. Left - z-coordinate of the maximum of the electric field $|\vec{\varepsilon}(r=0,z;t)|^{\max}$ on the axis versus time. Right - streamer velocity $V_s(t)$ versus time

For a plane - to - plane geometry, (1) and (2) represent the initial stage of an electron avalanche development, when the space charge is small, and the external electric field is not distorted by the space charge. The region (3) corresponds to the nonlinear stage of streamer propagation, when the magnitude of the space charge is significantly different from zero, and the external electric field is significantly distorted. The region (4) corresponds to the approach of the streamer to the anode, and to its exit through the anode from the simulation domain. Solution of the linearized equations (5) - (7) in one dimension, for the velocity of the ionization wave can be presented by:

$$V_a = |\varepsilon_0| + 2\sqrt{D|\varepsilon_0|\exp\left(-1/|\varepsilon_0|\right)}, \qquad (8)$$

where ε_0 is the external electric field, D is the diffusion coefficient. V_a is shown in Fig. 5 by a straight line. Fig. 5 shows that after a rather rapid transition process (region (1)) the streamer velocity V_s approaches the asymptotic velocity V_a (region (2)), which corresponds to the linear stage of the avalanche development.

In the case of non - uniform fields, the region (2) can not be identified as the linear stage of the avalanche development, because the effect of space charge appears much earlier. This follows directly from the analysis of potential distribution on the axis, which differs significantly from the vacuum potential distribution in the region (2) for each of the needle radii R_n = {20, 40, 80} and applied voltages V_0 = {96, 128, 160, 192}. Assuming that the speed of the streamer is determined by the electric field in the front of its head, it follows from the

simulations that $|\vec{\varepsilon}(r=0,z;t)|^{\max} \approx const$, and for $|\vec{\varepsilon}(r=0,z;t)|^{\max}$ in the region (2):

V_0	R	$\left\langle \|\vec{\varepsilon}\|^{\max} \right\rangle_{R_n}$	V_a^E
96	R =20,40,80	0.78	1.074
128	R =20,40,80	1.2	1.657
160	R =20,40,80	1.53	2.094
192	R =20,40,80	1.88	2.545

In the table, $\left\langle \|\vec{\varepsilon}\|^{\max} \right\rangle_{R_n}$ is the averaged over the needle radii electric field in the region (2), where the electric field $|\vec{\varepsilon}(r=0,z;t)|^{\max}$ and the speed of the streamer are slightly changed with time,

$$V_a^E = \left\langle |\vec{\varepsilon}|^{\max} \right\rangle_{R_n} + 2\sqrt{D\left\langle |\vec{\varepsilon}|^{\max} \right\rangle_{R_n}} e^{-\frac{1}{\left\langle |\vec{\varepsilon}|^{\max} \right\rangle_{R_n}}}. \quad (9)$$

The velocity V_a^E is shown in Fig. 5. As can be seen from Fig. 5, the negative streamer speed is well described by the expression (9).

Fig. 6 shows the velocity of the negative streamer V_s versus longitudinal coordinate z. It is seen that in the strong non-linearity regions (regions (3), and (4)) the speed of the streamer V_s as a function of longitudinal coordinate z is independent from the needle radius R_n. This can be explained by the screening of electric field of the needle by the space charge of the streamer.

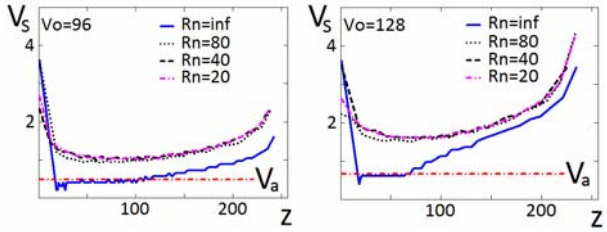

Fig. 6. Velocity of the negative streamer V_s versus longitudinal coordinate z for different needle radii R_n ={20, 40, 80, inf}, and different applied voltages V_0 = {96, 128}

Fig. 7 shows the streamer velocity V_s, for different applied voltages V_0 = {96, 128, 160, 192} with the constant needle radius R_n = {20, 40, 80, inf}. It is seen that as the applied voltage increases, the streamer velocity also increases.

Fig. 8 shows the streamer mean velocity $< V_s >$ as a function of the needle radius R_n ={20, 40, 80} for different applied voltages V_0 = {96, 128, 160, 192}. Mean velocity is defined as $< V_s >= L_z / \tau_{tr}$, where L_z is the discharge gap length, τ_{tr} is the passage time of the streamer through the discharge gap. It can be seen that the $< V_s >$ increases as R_n decreases at V_0 =const.

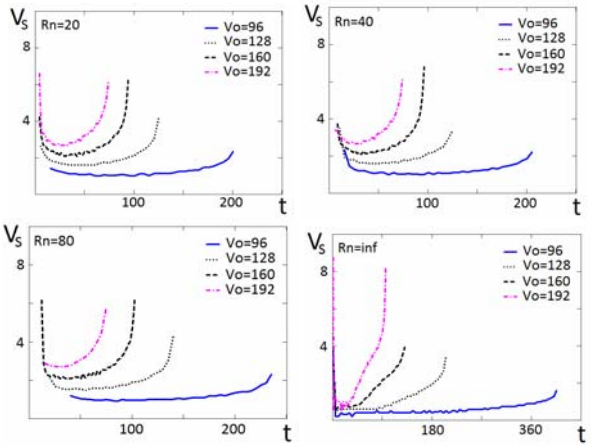

Fig. 7. Negative streamer dynamics for different applied voltages V_0 = {96, 128, 160, 192} and different radii of the needle R_n ={20, 40, 80, inf}. Streamer velocity $V_s(t)$ versus time

Starting from some R_n, the growth of streamer speed stops. It is also seen that $< V_s >$ increases with V_0.

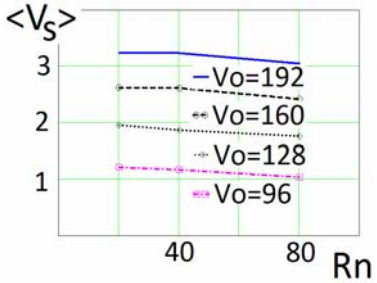

Fig. 8. The dependence of the negative streamer average speed $< V_s >$ on the radius of the needle R_n for different applied voltages V_0 = {96, 128, 160, 192}. R_n = {20, 40, 80}

Fig. 9 shows the streamer mean velocity $< V_s >$ as a function of the applied voltages V_0 ={96, 128, 160, 192} for different needle radii R_n ={20, 40, 80, inf}. It can be seen that the $< V_s >$ increases linearly with applied voltage V_0. It is seen also that the mean streamer velocity $< V_s >$ starting from certain R_n, does not depend on the needle radius R_n.

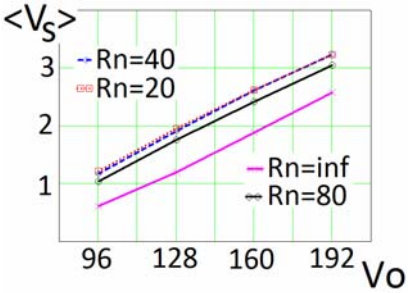

Fig. 9. The dependence of the negative streamer average speed $< V_s >$ on the applied voltage V_0 = {96, 128, 160, 192} for different radii of the needle R_n ={20, 40, 80}

ISSN 1562-6016. ВАНТ. 2013. №4(86)

CONCLUSIONS

The results of numerical simulations of the propagation of the negative streamer in nitrogen in the uniform and strongly non-uniform electric fields were presented. Computer simulations were performed by finite element method, which allows to accurately describe the boundaries of complicated shape. Simulations were done for different voltages, and for different radii of the needles.

It was shown that the velocity of streamer propagation in the non - uniform electric field is always higher than the velocity of streamer propagation in the uniform field at given voltages on the electrodes.

It was shown that the behavior of streamer velocity versus time has four specific regions: (1) the sharp drop at the beginning of the movement, (2) the propagation with a constant velocity, (3) the region of the first (low) acceleration, and (4) the area of the second (strong) acceleration when the streamer head approaches the anode.

It was shown that as the needle radius decreases, the velocity of the streamer increases. The growth of streamer velocity, with decreasing needle radius, is stopped when the needle curvature radius reaches a certain critical size.

It was shown that in the region of strong nonlinearity, namely, in the space charge dominated region, the streamer velocity as the function of longitudinal coordinate is independent from the needle radius. It was shown that the streamer velocity increases with growth of the applied voltage.

REFERENCES

1. A.A. Kulikovsky. The structure of streamers in N2. I. fast method of space-charge dominated plasma simulation // *J. Phys. D: Appl. Phys.* 1994, v. 27, p. 2556-2563.
2. A.A. Kulikovsky. The structure of streamers in N2. II. Two-dimensional simulation // *J. Phys. D: Appl. Phys.* 1994, v. 27, p. 2564-2569.
3. A.A. Kulikovsky. Two-dimensional simulation of the positive streamer in N2 between parallel-plate electrodes // *J. Phys. D: Appl. Phys*. 1995, v. 28, p. 2483-2493.
4. M. Arrayás, U. Ebert, W. Hundsdorfer. Spontaneous branching of anode-directed streamers between planar electrodes // *Phys. Rev. Lett.* 2002, v. 88, p. 174502.
5. C. Montijn, W. Hundsdorfer, U. Ebert. An adaptive grid refinement strategy for the simulation of negative streamers // *J. Comp. Phys.* 2006, v. 219, p. 801-835.
6. A.A. Kulikovsky. A more accurate Scharfetter-Gummel algorithm of electron transport for semiconductor and gas discharge simulation // *J. Comp. Phys.* 1994, v. 119, p. 149-155.
7. V.I. Golota, Yu.V. Dotsenko, V.I. Karas', O.V. Manuilenko, A.S. Pismenetskii. Simulation of negative streamer in nitrogen // *Problems of Atomic Science and Technology. Ser. «Plasma Electronics and New Meth. of Accel» (7)*. 2010, № 4, p. 176-180.
8. O.V. Manuilenko, V.I. Golota. Particularities of the negative streamer propagation in homogeneous and inhomogeneous electric fields // *Problems of Atomic Science and Technology. Ser. «Plasma Physics» (83)*. 2013, № 1, p. 171-173.

Article received 29.04.2013.

ЧИСЛЕННОЕ МОДЕЛИРОВАНИЕ ОТРИЦАТЕЛЬНЫХ СТРИМЕРОВ В СИЛЬНЫХ НЕОДНОРОДНЫХ ЭЛЕКТРИЧЕСКИХ ПОЛЯХ В АЗОТЕ. ВЛИЯНИЕ РАДИУСА ИГЛЫ И ПРИЛОЖЕННОГО НАПРЯЖЕНИЯ НА СКОРОСТЬ СТРИМЕРА

О.В. Мануйленко, В.И. Голота

Приведены результаты численного моделирования распространения отрицательного стримера в азоте в однородных и сильно неоднородных электрических полях. Показано, что скорость распространения стримера в неоднородном поле всегда больше его скорости в однородном поле при одинаковых потенциалах на электродах. Показано, что при уменьшении радиуса иглы скорость стримера увеличивается при заданном напряжении на электродах. Рост скорости стримера, с уменьшением радиуса иглы, прекращается, когда радиус кривизны иглы достигает некоторого критического размера. Показано, что в области сильной нелинейности, когда динамика распространения стримера определяется его объемным зарядом, его скорость, как функция продольной координаты не зависит от радиуса иглы. Показано, что скорость стримера возрастает с ростом напряжения, приложенного к электродам.

ЧИСЛОВЕ МОДЕЛЮВАННЯ НЕГАТИВНИХ СТРИМЕРІВ У СИЛЬНИХ НЕОДНОРІДНИХ ЕЛЕКТРИЧНИХ ПОЛЯХ В АЗОТІ. ВПЛИВ РАДІУСА ГОЛКИ І ПРИКЛАДЕНОЇ НАПРУГИ НА ШВИДКІСТЬ СТРИМЕРА

О.В. Мануйленко, В.І. Голота

Наведено результати числового моделювання поширення негативного стримера в азоті в однорідних і сильно неоднорідних електричних полях. Показано, що швидкість поширення стримера в неоднорідному полі завжди більша його швидкості в однорідному полі при однакових потенціалах на електродах. Показано, що при зменшенні радіуса голки швидкість стримера збільшується при заданій напрузі на електродах. Зростання швидкості стримера, із зменшенням радіуса голки, припиняється, коли радіус кривизни голки досягає деякого критичного розміру. Показано, що в області сильної нелінійності, коли динаміка поширення стримера визначається його об'ємним зарядом, його швидкість, як функція поздовжньої координати не залежить від радіуса голки. Показано, що швидкість стримера зростає з ростом напруги, що прикладена до електродів.